Cell, Vol. 123, 697–709, November 18, 2005, Copyright ©2005 by Elsevier Inc. DOI 10.1016/j.cell.2005.08.038

stathmin, a Gene Enriched in the Amygdala, Controls Both Learned and Innate Fear

Gleb P. Shumyatsky,[1,*] Gaël Malleret,[2] Ryong-Moon Shin,[3] Shuichi Takizawa,[1] Keith Tully,[3] Evgeny Tsvetkov,[3] Stanislav S. Zakharenko,[2,5] Jamie Joseph,[1] Svetlana Vronskaya,[2] DeQi Yin,[2] Ulrich K. Schubart,[4] Eric R. Kandel,[2] and Vadim Y. Bolshakov[3]

[1]Department of Genetics
Rutgers University
Piscataway, New Jersey 08854
[2]Howard Hughes Medical Institute
Center for Neurobiology and Behavior
Columbia University
New York, New York 10032
[3]McLean Hospital
Department of Psychiatry
Harvard Medical School
Belmont, Massachusetts 02478
[4]Department of Medicine
Albert Einstein College of Medicine
Bronx, New York 10461

Summary

Little is known about the molecular mechanisms of learned and innate fear. We have identified stathmin, an inhibitor of microtubule formation, as highly expressed in the lateral nucleus (LA) of the amygdala as well as in the thalamic and cortical structures that send information to the LA about the conditioned (learned fear) and unconditioned stimuli (innate fear). Whole-cell recordings from amygdala slices that are isolated from *stathmin* knockout mice show deficits in spike-timing-dependent long-term potentiation (LTP). The knockout mice also exhibit decreased memory in amygdala-dependent fear conditioning and fail to recognize danger in innately aversive environments. By contrast, these mice do not show deficits in the water maze, a spatial task dependent on the hippocampus, where stathmin is not normally expressed. We therefore conclude that stathmin is required for the induction of LTP in afferent inputs to the amygdala and is essential in regulating both innate and learned fear.

Introduction

There is increasing evidence that many aspects of memory in the mammalian brain involve cellular and molecular events that are directed by gene expression that is neural circuitry specific (Rodrigues et al., 2004; Tonegawa et al., 2003). To relate learning and memory to specific genes in specific neural circuitry, it is useful first to focus on simple neural circuitry of the sort involved in forms of implicit memory storage.

Within the mammalian brain, one of the best understood memory-related neural circuitries is that which controls fear conditioning. Fear reactions represent not a single process but a spectrum of behaviors that vary from those that are inborn to those that are acquired. The expression of inborn (innate) fear needs no previous experience and is often species specific toward actual or potential threats (for example, fear of heights and predator or predator-like shadow avoidance). In contrast, acquired (learned) fear is the result of experiencing certain aversive or life-threatening events in the past (for example, school avoidance by child as a result of being the victim of a bully). Because it is so essential for survival, memory for fear is easily established, very resistant to extinction, and normally lasts for the duration of the animal's lifetime.

In the neural circuitry responsible for auditory fear conditioning, memory is formed as an association between a neutral conditioned stimulus (such as an auditory tone, CS) and an aversive unconditioned stimulus (electric footshock, US), which occurs in the lateral nucleus (LA) of the amygdala (Fendt and Fanselow, 1999; LeDoux, 2000; Maren and Quirk, 2004). The auditory information about the CS is transmitted to the LA by way of two projections, the thalamo-amygdala and cortico-amygdala pathways. The direct thalamo-amygdala pathway projects from the medial division of the medial geniculate nucleus (MGm) and the posterior intralaminar nucleus (PIN) of the auditory thalamus. The indirect cortico-amygdala pathway consists of the projections originating in the auditory thalamus that relay auditory information to the TE3 area of the auditory cortex and then to the LA.

In contrast to the neuroanatomic circuitry responsible for the CS, the routes by which US information is transmitted to the amygdala are not well understood (Davis, 2000; Fendt and Fanselow, 1999; McGregor et al., 2004). Anatomic tracing and lesion studies suggest that there are several pathways providing the amygdala with nociceptive input (Brunzell and Kim, 2001; Campeau and Davis, 1995; Lanuza et al., 2004; Shi and Davis, 1999). The somatosensory information comes from the somatosensory thalamus and cortex and possibly some other fibers located medial to the posterior thalamus. The thalamic areas that carry information about the US include the paraventricular nucleus (PV); the reuniens nucleus; the ventral posteromedial (VPM) and the ventral posterolateral (VPL) nuclei; and the posterior intralaminar thalamic complex that contains the PIN, the medial geniculate nucleus (MGN) and the suprageniculate nucleus (SG). The cortical areas carrying US information include the S1 and S2 of the somatosensory complex, the parietal insular cortex (PaIC), and the perirhinal cortex (PRh). Thus, the anatomic circuitries carrying information about the CS and US may substantially overlap before they converge in the amygdala. Interestingly, learned-fear behavior can be genetically manipulated independent of innate fear (Shumyat-

*Correspondence: gleb@biology.rutgers.edu
[5]Present address: Department of Developmental Neurobiology, St. Jude Children's Research Hospital, Memphis, Tennessee 38017.

sky et al., 2002), which suggests that the neural circuitries for innate and learned fear might be present as separate functional entities within those afferent regions carrying the CS and US.

The relative simplicity of fear conditioning as a training paradigm and the well-defined neuroanatomic circuitry for the CS make learned fear amenable to the cellular physiological and molecular analyses. As a first step to unravel the molecular events underlying fear learning, we have recently identified several amygdala-enriched genes (Shumyatsky et al., 2002). Here we describe the role in fear of an amygdala-enriched gene called *stathmin/oncoprotein 18* (Shumyatsky et al., 2002). Stathmin is a cytosolic phosphoprotein (Hanash et al., 1988) that interacts with tubulin heterodimers and prevents them from forming microtubules (MTs) (Curmi et al., 1997). After phosphorylation, stathmin releases tubulin, allowing MT formation. Stathmin is involved in MT dynamics by regulating both the formation of MT and their disassembly (Belmont and Mitchison, 1996).

We now have characterized the expression pattern of stathmin in the neural circuitry of fear in the adult mouse brain and analyzed the consequences of stathmin ablation for amygdala long-term potentiation (LTP) and fear behavior in *stathmin* knockout mice. We have found that LTP in the LA as well as learned and innate fear are controlled by stathmin expression in the LA and its sensory afferent projections.

Results

The Lateral Nucleus of the Amygdala and Its Afferents Are Enriched in Stathmin

We have previously described the differential screening of single-cell cDNA libraries derived from individual principal cells in the LA that allowed us to identify the expression of the genes encoding gastrin-releasing peptide (*Grp*) and *stathmin* as highly enriched in the amygdala (Shumyatsky et al., 2002). In the adult mouse (3 months old), stathmin expression is limited to brain and testis (Schubart et al., 1992). We found stathmin to be present in several nuclei of the amygdala, such as the LA, basolateral (BLA), and basomedial (BMA) nuclei; its expression was particularly strong in the LA (Figures 1A and 1C). In the LA, stathmin was strongly expressed in the dorsolateral and dorsomedial divisions and to a lesser extent in its dorsoventral division. Stathmin was also expressed in the regions known to process US and CS information before it reaches the LA. The CS areas included the PIN, the MGN, and the SG of the auditory thalamus (Figure 1B) and the TE3 area of the auditory cortex (Figure 1A). Stathmin was also localized in the perirhinal cortex (PRh, Figure 1A), which is considered to be a multimodal associative complex that can transmit auditory and visual CS as well as somatosensory US information. Other US areas included the ventral posterolateral thalamic nucleus (LP), the paraventricular (PV) thalamic nucleus, and the reuniens (Re) thalamic nucleus (Figure 1A). Stathmin was also localized in the S1 and S2 areas of the somatosensory cortex, the parietal cortex, and the parietal insular cortex. Thus, stathmin is expressed in brain areas that were previously described as relaying US and CS projections to the amygdala (Figure 1E). Other areas of stathmin expression were the endopiriform cortex and the piriform cortex that are adjacent and reciprocally connected to the amygdala (Majak et al., 2002). Consistent with the previous observations (Amat et al., 1991), stathmin was weakly expressed in the dentate gyrus and was absent from the rest of the hippocampus (Figure 1A).

We also compared the expression of *stathmin* in newborn, 2-week-old, and 2-month-old mice (Figure 1D). The *stathmin* gene was expressed in many areas of the newborn brain, but its expression declined in juvenile and even more so in adult brain, where *stathmin* remained expressed only in the amygdala and in its US and CS pathways.

To determine the identity of cells that express stathmin in the amygdala, we compared stathmin localization with that of the markers of different cell types. We first examined stathmin presence in neuronal cells by studying its colocalization with antibody against NeuN protein, a marker of mature neurons that is expressed both in principal cells and interneurons. In the amygdala, the majority of cells labeled by both anti-NeuN antibody and by anti-stathmin antibody colocalized (Figures 2Aa–2Ac). In the striatum, we found only cells labeled by anti-NeuN antibody, confirming our in situ hybridization experiments (Figures 1A) that show stathmin absence from the striatum. We next found that stathmin was mainly present in principal cells positive for CaMKIIα (Figures 2Ba–2Bc), a marker of excitatory principal cells (McDonald et al., 2002). A few cells were labeled by only one type of the antibody and not by another (Figure 2Bc, white arrows), and we roughly estimated that more than 90% of cells, expressing stathmin or CaMKIIα, overlap. Colocalization experiments with antibody against anti-GFAP (glial fibrillary acidic protein), a marker of glial cells, showed that stathmin was not expressed in glia (Figures 2Ca-2Cc). Stathmin therefore is expressed mostly in pyramidal neurons in the LA and the BLA, potentially affecting MT formation in the excitatory principal cells in these areas.

Increased Amount of Microtubules in the Amygdala of *stathmin* Knockout Mice

To begin to assess stathmin function in the amygdala, we examined the consequences of stathmin deletion on MT formation in *stathmin* knockout mice. Mice without stathmin develop normally and show no obvious anatomical abnormalities throughout their body, including brain (Schubart et al., 1996). Western blotting using amygdala tissue showed that stathmin protein was absent in *stathmin* knockout animals (Figure 3A).

Using an MT in vivo binding assay (Marklund et al., 1996), we analyzed the amount of tubulin in polymerized MTs (Figure 3Ab). The amount of α-tubulin in the MT fraction was increased 50% in the mutant mice (KO) compared to their controls (wild-type) (20 repeats, 3 mice; significant difference between groups, t test, $p < 0.02$; Figure 3B). We found equal amounts of glyceraldehyde-3-phosphate dehydrogenase (GAPDH; Figure 3Ac) in the samples of both wild-type and knockout mice (8 repeats, 3 mice; no significant difference between groups, t test, $p = 0.5$; Figure 3Ac). The increased

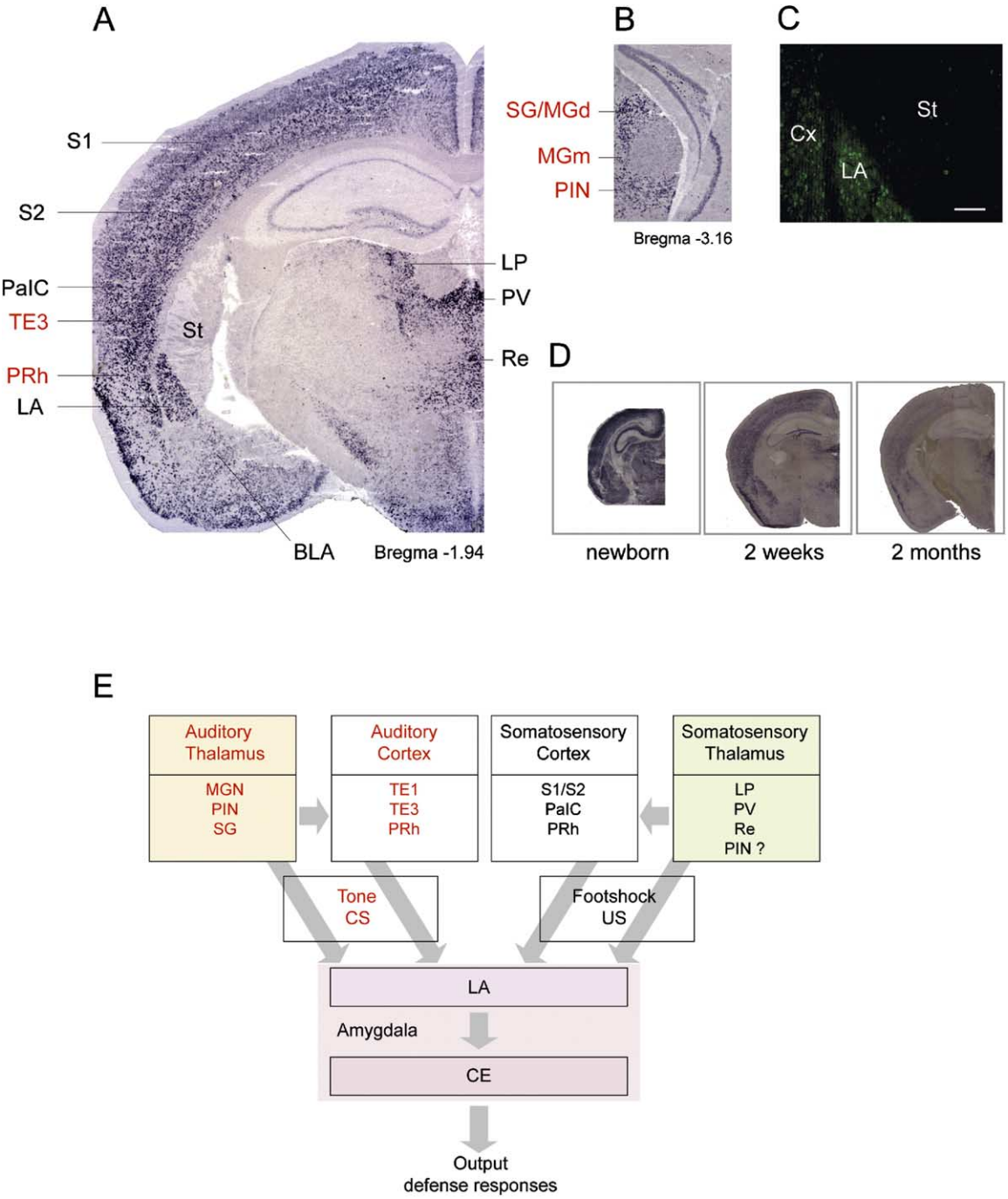

Figure 1. Expression of *stathmin* Gene in the Mouse Brain

(A) Expression of *stathmin* RNA in the amygdala, cortical, and thalamic areas. S1, primary somatosensory cortex; S2, secondary somatosensory cortex; PaIC, parietal insular cortex; TE3, temporal cortex area 1; LA, lateral nucleus of the amygdala; BLA, basolateral nucleus of the amygdala; PRh, perirhinal cortex; LP, lateral posterior thalamic nucleus; PV, paraventricular thalamic nucleus; Re, reuniens thalamic nucleus.

(B) Expression of *stathmin* RNA in the auditory thalamus. SG, suprageniculate nucleus; MGd, dorsal division of the medial geniculate nucleus (MGN); MGm, medial division of the MGN; PIN, posterior intralaminar nucleus.

(C) Staining with anti-stathmin antibody demonstrates lack of expression of stathmin protein in the striatum (St). Cx, cerebral cortex. Bar is 100 μm.

(D) Expression of *stathmin* RNA in the postnatal mouse brain.

(E) Major neural pathways transmitting tone CS and foot-shock US to the amygdala. Areas in red transmit CS to the LA; areas in black transmit US to the LA. Gray arrows show the direction of sensory information. Abbreviations are as in (A) and (B). CE, central nucleus of the amygdala.

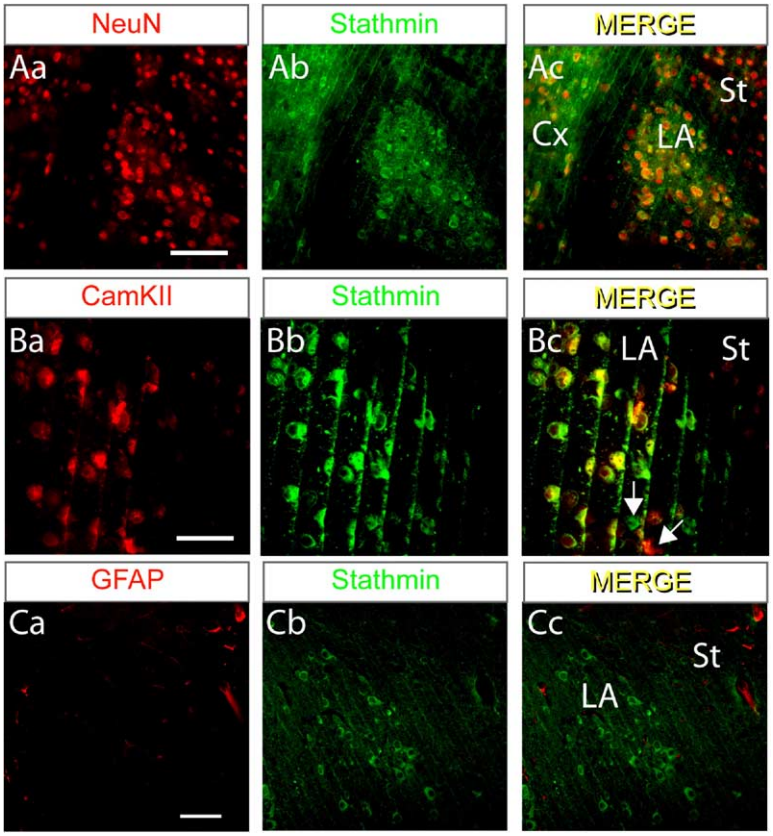

Figure 2. Expression of Stathmin in Neurons

(Aa–Ac) Stathmin is localized in neurons labeled by NeuN antibody, a marker of mature neurons. (Aa) shows expression of NeuN; (Ab) shows expression of stathmin. Scale bar is 50 μm.

(Ba–Bc) Cells expressing stathmin are positive for CaMKIIα antibody, a marker of pyramidal neurons. (Ba) shows expression of CaMKIIα; (Bb) shows stathmin. White arrows show examples of cells that do not colocalize. Scale bar is 25 μm.

(Ca–Cc) Stathmin is not expressed in glial cells. (Ca) shows expression of glia marker GFAP; (Cb) shows expression of stathmin. Scale bar is 50 μm.

level of polymerized tubulin suggests that the rate of MT dynamics may be downregulated in *stathmin* knockout mice, leading to MTs that stay longer in the assembled form.

To analyze possible effects of increased MT stability on brain function in *stathmin* knockout mice, we first examined whether MTs and stathmin are present in synapse. We found that both MTs and stathmin are localized in the synaptosomal fraction (SN) that was isolated from wild-type mouse brain (Figures 3Ba and 3Bb). Synaptic protein markers synaptophysin, PSD-95, and CaMKII were enriched in the SN, and the high-molecular-weight form of microtubule-associated protein (MAP2) was absent from the SN, thus demonstrating that the synaptosomal fraction was successfully isolated. The finding that MTs and stathmin are present in synapse is consistent with the previously published work and confirms that MTs are present to some extent in dendritic spines (Gavet et al., 2002; Kaech et al., 2001; van Rossum and Hanisch, 1999).

To examine whether *stathmin* deletion influenced the basal morphological characteristics of pyramidal neurons, we used two-photon imaging in *stathmin* knockout mice that carried the *Thy1-EGFP* transgene (M line) randomly expressing EGFP throughout the nervous system (Feng et al., 2000). Pyramidal neurons were identified by presence of dendritic spines on apical dendrites and the distinguishing cell body shape. We could not find any obvious changes in morphology of pyramidal neurons in *stathmin*$^{-/-}$*/Thy1-EGFP* mice compared to *stathmin*$^{+/+}$*/EGFP* mice (Figures 3Ca and 3Cb). In the LA, spine density was 0.51 ± 0.05 μm^{-1} in *stathmin*$^{-/-}$*/EGFP* mice (n = 18 neurons) compared to 0.64 ± 0.04 μm^{-1} in wild-type littermates (n = 21 neurons, $p > 0.05$, Kolmogorov-Smirnov test). Similarly, in the hippocampus, where *stathmin* expression is negligible, pyramidal neurons were not affected in the knockouts. Spine density in CA1 pyramidal neurons was 1.20 ± 0.08 μm^{-1} (n = 21 neurons, 2 mice) and 1.20 ± 0.1 μm^{-1} (n = 10, $p > 0.05$, Kolmogorov-Smirnov test) in *stathmin*$^{-/-}$*/EGFP* and *stathmin*$^{+/+}$*/EGFP* mice, respectively. We thus conclude that neuronal morphology is normal in *stathmin* knockout mice.

Synaptic Transmission in the Cortico-Amygdala and Thalamo-Amygdala Pathways Is Normal in *stathmin* Knockout Mice

To explore the possible effects of *stathmin* deletion on synaptic transmission in afferent inputs to the LA that carry auditory signals essential for learned fear, we recorded compound excitatory postsynaptic currents (EPSCs) in pyramidal cells in the LA, evoked by stimulation of either the external capsule (cortical input; Figure 4A, left) or the internal capsule (thalamic input; Figure 4A, right) in the presence of the γ-aminobutyric acid-A ($GABA_A$) receptor antagonist picrotoxin (50 μM). Recorded cells were identified as pyramidal neurons based on their ability to show spike frequency adaptation in response to the prolonged depolarizing-current injections (Mahanty and Sah, 1998; Tsvetkov et al., 2002, 2004).

We found no differences between experimental

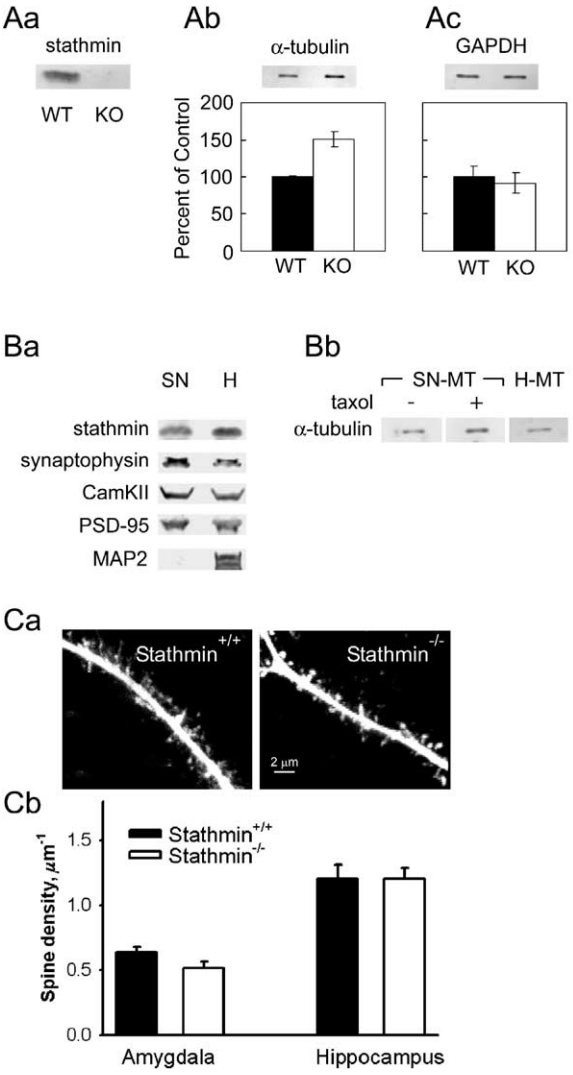

Figure 3. Increased Level of Microtubules in the Amygdala of *stathmin* Knockout Mice

(Aa) Stathmin protein is absent in the amygdala of *stathmin* knockout mice.

(Ab) The amount of α-tubulin is increased in the MT fraction of *stathmin* knockout mice. Error bars indicate SD.

(Ac) The amount of GAPDH protein is normal in *stathmin* knockout mice. KO, *stathmin* knockout mice; WT, wild-type mice. Error bars indicate SD.

(Ba and Bb) Stathmin and MTs are present in the synaptosomal fraction (SN) of the mouse brain.

(Ba) Stathmin is present in the SN. Synaptic protein markers synaptophysin, CaMKII, and PSD-95 are enriched and MAP2 is absent in the synaptosomal fraction. Whole-cell lysate is loaded as a control (H).

(Bb) α-tubulin from the MT fraction (MT) is enriched in the synaptosomal fractions isolated with Taxol (+) and without Taxol (–). The same protein amount of amygdala pellet fraction containing MT-formed α-tubulin was also loaded as a control (H-MT). SN-MT, pellet fraction containing MT-formed tubulin from the synaptosomal fraction; H-MT, pellet fraction containing MT-formed tubulin from amygdala homogenate.

(Ca and Cb) Dendritic-tree morphology is preserved in *stathmin* knockout mice

(Ca) A part of a dendritic tree visualized in EGFP-expressing neurons in LA from *stathmin*$^{+/+}$*/Thy1-EGFP* (left panel) and *stathmin*$^{-/-}$*/Thy1-EGFP* mice (right panel).

(Cb) Average spine density in dendrites from the LA and the hippocampus from *stathmin*$^{+/+}$*/Thy1-EGFP* (black) and *stathmin*$^{-/-}$*/Thy1-EGFP* mice (white). Error bars indicate SEM.

groups in synaptic input-output curves, which provide an integral measure of synaptic strength at either cortico-amygdala synapses (Figure 4B; 8 cells, obtained from 4 control mice, and 13 cells, obtained from 4 knockout mice; no significant difference, two-way ANOVA, p = 0.83) or thalamo-amygdala synapses (Figure 4E; 8 cells, obtained from 4 control mice, and 11 cells, obtained from 4 knockout mice; no significant difference, two-way ANOVA, p = 0.61).

Paired-pulse facilitation (PPF) of the EPSC, which is a mostly presynaptic phenomenon, was also not affected in *stathmin*-deficient mice in either pathway (Figures 4C, 4D, 4F, and 4G). Thus, PPF at a 50 ms interstimulus interval in cortical input was 1.32 ± 0.05 (7 cells, 3 mice) in slices from control mice compared with 1.3 ± 0.1 in slices from *stathmin* knockout mice (9 cells, 3 mice; no significant difference, t test, p = 0.65). PPF in thalamic input was 1.22 ± 0.1 (8 cells, 4 mice) in slices from control mice compared with 1.21 ± 0.05 in slices from *stathmin* knockout mice (11 cells, 4 mice; no significant difference, t test, p = 0.81). This indicates that deletion of stathmin does not lead to changes in Ca^{2+}-dependent transmitter release.

To further characterize the role of stathmin in synaptic transmission, we recorded glutamatergic miniature EPSCs (mEPSCs) in the LA pyramidal neurons in the presence of tetrodotoxin (1 μM) to block action-potential firing. These currents reflect spontaneous release of single quanta of neurotransmitter that is at least partially Ca^{2+} independent. The frequency of mEPSCs was 3.98 ± 0.97 Hz (4 cells, obtained from 4 mice) in control mice and 3.3 ± 0.7 Hz (4 cells, obtained from 3 mice) in *stathmin* knockout mice (Figures 4H–4J; no significant difference, t test, p = 0.58). This implies that stathmin is not required for either Ca^{2+}-dependent or Ca^{2+}-independent transmitter release under baseline conditions. The sensitivity of the postsynaptic α-amino-3-hydroxy-5-methyl-4-isoxazolepropionic acid (AMPA) receptors to glutamate was also unchanged in mutant mice. Thus, mean mEPSC amplitudes in control and knockout mice were 8.1 ± 0.7 pA (4 cells, obtained from 4 mice) and 7.05 ± 1.5 pA (4 cells, obtained from 3 mice), respectively (Figures 4H–4J; no significant difference, t test, p = 0.54). These findings are consistent with the notion that basal excitatory synaptic transmission is not affected in mutant mice.

We also investigated whether ablation of *stathmin* gene results in changes of GABA-mediated inhibition in the LA. First, we recorded inhibitory postsynaptic currents (IPSCs) in the pyramidal neurons at a holding potential of –70 mV in the presence of the AMPA-receptor (AMPAR) antagonist 6-cyano-7-nitroquinoxaline-2,3-dione (CNQX, 20 μM) using a chloride-based intrapipette solution. In these experiments, the stimulation electrode was placed within the LA to directly activate interneurons. The analysis of the input-output curves for the monosynaptic GABAergic IPSC revealed no differences between control (15 cells, obtained from 4

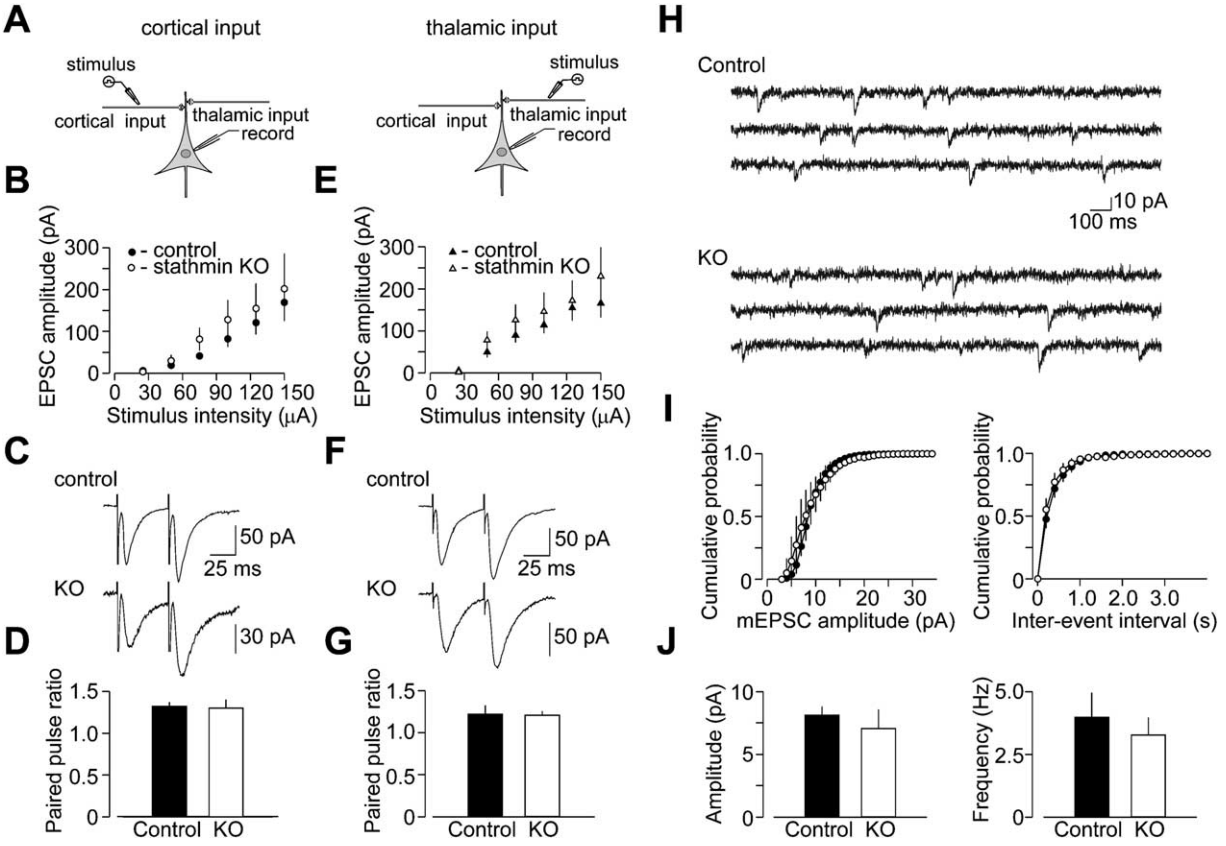

Figure 4. Basal Synaptic Transmission at the Cortico-Amygdala and Thalamo-Amygdala Inputs to the LA Is Normal in *stathmin* Knockout Mice

Error bars indicate SEM.

(A) A schematic representation of the experimental design showing the position of the recording and stimulation electrodes.

(B) Synaptic input-output curves obtained in the cortical input to the LA in slices from control (●) and *stathmin* knockout (○) mice. The EPSC amplitude is plotted as a function of stimulation intensity.

(C) Examples of paired-pulse facilitation of the cortico-amygdala EPSC recorded at a 50 ms interstimulus interval in control (upper) and mutant (lower) synapses. Traces show average of 10 responses. Paired-pulse facilitation was calculated as the ratio of the second EPSC amplitude to the first EPSC amplitude.

(D) Summary plot of paired-pulse-facilitation experiments in the cortical input to the LA.

(E) Synaptic input-output curves obtained in the thalamic input to the LA in slices from control (▲) and *stathmin* knockout (△) mice. The EPSC amplitude is plotted as a function of stimulation intensity.

(F) Examples of paired-pulse facilitation of the thalamo-amygdala EPSC recorded at a 50 ms interstimulus interval in control (upper) and mutant (lower) synapses. Traces show average of 10 responses.

(G) Summary plot of paired-pulse-facilitation experiments in the thalamic input to the LA.

(H) Representative mEPSCs recorded in the LA neuron in slices from control (upper) and knockout (lower) mice at a holding potential of −70 mV.

(I) Cumulative amplitude (left) and interevent interval (right) histograms of mEPSCs recorded in slices from control (●) and *stathmin* knockout (○) mice.

(J) Summary plots of mEPSC data. Averaged values of mEPSC parameters, mean peak amplitude (left) and frequency (right).

control mice) and knockout mice (13 cells, obtained from 4 knockout mice; ANOVA, p = 0.76; Figures 5A–5C). Second, to characterize the effect of mutation on tonic inhibition in the LA, we recorded spontaneous IPSCs (sIPSCs) in the LA neurons from control and knockout mice in the presence of CNQX. We found that deletion of stathmin had no effect on either the frequency or amplitude of sIPSCs. Thus, the frequency of sIPSCs was 1.57 ± 0.3 Hz (11 cells, obtained from 4 mice) in control mice and 1.77 ± 0.3 Hz (12 cells, obtained from 4 mice) in *stathmin* knockout mice (Figures 5D–5F; no significant difference, t test, p = 0.66). The mean sIPSC amplitude in control and knockout mice was 47.7 ± 5.4 pA (11 cells, obtained from 4 mice) and 47.0 ± 6 pA (12 cells, obtained from 4 mice), respectively (Figures 5E and 5F; no significant difference, t test, p = 0.9). These data indicate that $GABA_A$-receptor-mediated inhibition is normal in *stathmin* knockout mice.

LTP in the Cortico-Amygdala and Thalamo-Amygdala Pathways Is Impaired in Mice Lacking Stathmin

Recent findings suggest a direct causal link between long-term synaptic enhancements in the pathways that transmit auditory signals to the LA and fear learning (Tsvetkov et al., 2002). The *stathmin* gene is highly en-

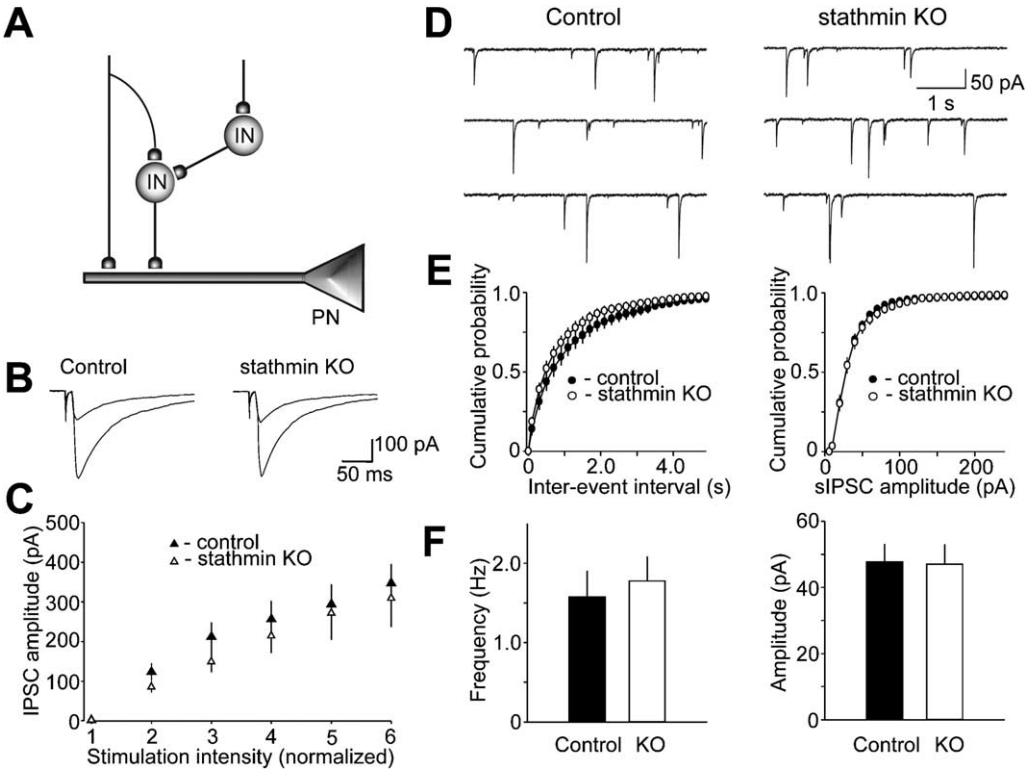

Figure 5. $GABA_A$ Receptor-Mediated Inhibition of Principal Neurons in the LA Is Normal in *Stathmin* Knockout Mice

Error bars indicate SEM.

(A) A schematic representation of the neural circuit for $GABA_A$R inhibition in the LA. PN, principal neuron; IN, interneuron.

(B) Examples (average of 10 events) of IPSCs evoked by stimulation pulses of two different intensities (see [C] for details) obtained from individual experiments in slices from control (left) or *stathmin* knockout (right) mice.

(C) Synaptic input-output curves for the $GABA_A$R IPSCs obtained in slices from control (▲) and *stathmin* knockout (△) mice. The IPSCs were elicited by the stimulation electrode placed within the LA and recorded from the principal cell at a holding potential of −70 mV. The intensity of stimulation was gradually increased from the threshold stimulus, determined in each individual experiment, with an increment of 25 μA to produce IPSCs of increasing amplitude. The IPSC amplitude (mean ± SEM) is plotted as a function of stimulation intensity.

(D) Representative sIPSCs recorded in the LA neuron in slices from control (left) and knockout (right) mice at a holding potential of −70 mV.

(E) Cumulative interevent interval (left) and amplitude (right) histograms of sIPSCs recorded in slices from control (●) and *stathmin* knockout (○) mice. From 800 to 1200 sIPSCs were recorded and analyzed in each individual experiment.

(F) Summary plots of sIPSC data. Averaged values of sIPSC parameters, frequency (left) and mean peak amplitude (right).

riched in the LA (Figure 1) and is specifically expressed by the LA principal cells. It prompted us to investigate whether stathmin is required for LTP in afferent inputs to the LA, thus potentially affecting fear behavior.

We examined in a blinded fashion LTP of the compound excitatory postsynaptic potentials (EPSPs), recorded in current-clamp mode at the cortico-amygdala or thalamo-amygdala synapses in slices from control or *stathmin* knockout mice. LTP was induced by pairing of 80 presynaptic stimuli, delivered to the fibers in either the external capsule (cortical input) or the internal capsule (thalamic input) at a frequency of 2 Hz, with action potentials that were evoked in the postsynaptic cell with 4–6 ms delay from the onset of each EPSP by current injection through the recording electrode. LTP was recorded in the presence of the $GABA_A$-receptor antagonist picrotoxin (50 μM). We found that LTP in both pathways was significantly reduced in knockout as compared with control mice (Figures 6A–6D). When measured 35–40 min after LTP-inducing stimulation, the cortico-amygdala EPSP was potentiated to 148% ± 8.7% of its initial value in control mice (6 cells, obtained from 4 control mice) and to 114% ± 10.1% of its baseline value in *stathmin* knockout mice (7 cells, obtained from 5 knockout mice; significant difference, t test, $p < 0.03$). In thalamic input, the EPSP was potentiated to 154.4% ± 20% of its initial value in control mice (6 cells, obtained from 4 control mice) and remained at 93% ± 3% of its baseline value in *stathmin* knockout mice (7 cells, obtained from 4 knockout mice; significant difference, t test, $p < 0.02$). Thus, stathmin is necessary for the induction of timing-based, associative LTP of glutamatergic synapses in the LA.

We also addressed a question of whether downregulation of the rate of MT dynamics in *stathmin* knockout mice (see Figure 3) is related to the observed LTP deficit. We tested the effects of paclitaxel (10 μM; slices were pretreated for at least 30 min), which binds to MTs and inhibits their depolymerization, on LTP in slices from wild-type mice. Under these conditions, LTP was significantly reduced when assessed 35–40 min after

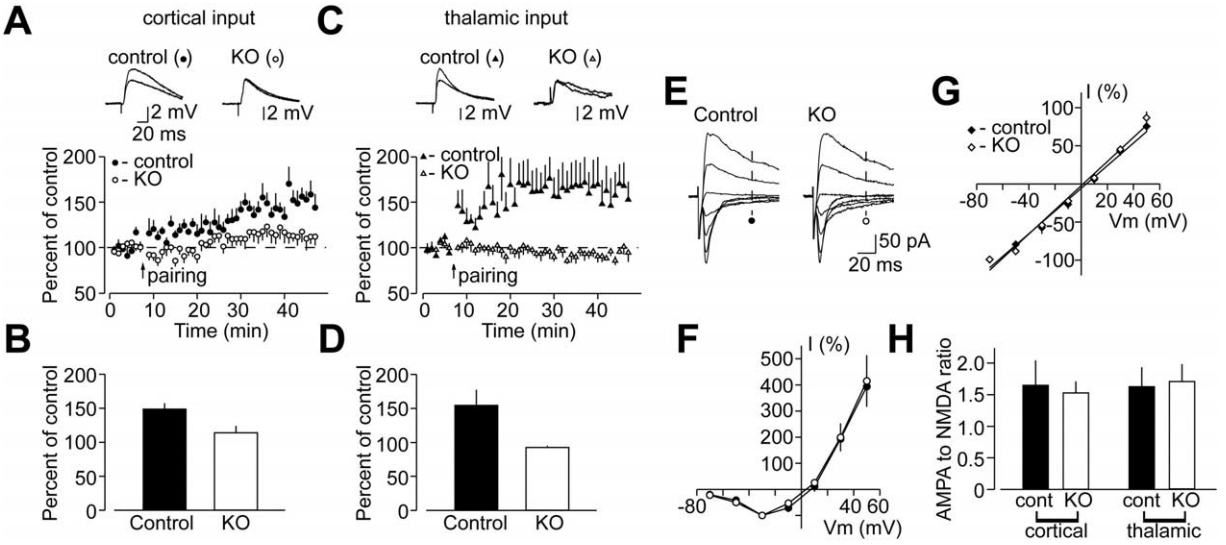

Figure 6. LTP at the Cortico-Amygdala and Thalamo-Amygdala Synapses Is Impaired in *stathmin* Knockout Mice

Error bars indicate SEM.

(A) AP-EPSP pairing-induced LTP of the cortico-amygdala EPSP recorded in the LA neuron in slices from control (●) or *stathmin* knockout (○) mice. Insets show the average of ten EPSPs recorded before and 35 min after the pairing procedure (arrow) in slices from control (left) and knockout (right) mice.

(B) Summary of LTP experiments at the cortico-amygdala pathway in control and knockout mice.

(C) LTP of the thalamo-amygdala EPSP recorded in the LA neuron in slices from control (▲) or *stathmin* knockout (△) mice. Traces show the average of ten EPSPs recorded before and 35 min after the pairing procedure (arrow).

(D) Summary of LTP experiments at the thalamo-amygdala pathway in control and knockout mice.

(E) EPSCs evoked by the stimulation of the external capsule at holding potentials ranging from −70 mV to +50 mV in slices from control (left) and *stathmin* knockout (right) mice. Traces are averages of ten EPSCs recorded at each holding potential.

(F) Current-voltage plot of the NMDAR-mediated cortico-amygdala EPSCs measured 50 ms after the peak AMPAR EPSC in control (●) and knockout (○) mice. Values for the graph were obtained by normalizing the mean NMDAR current at each holding potential to the mean NMDAR EPSC recorded at a holding potential of −30 mV.

(G) Current-voltage plot of the peak current mediated by the AMPA receptors in slices from control (●) and knockout (○) mice. Values for the graph were obtained by normalizing the mean AMPAR peak current at each holding potential to the mean amplitude of the AMPAR EPSC recorded at a holding potential of −70 mV.

(H) AMPA/NMDA receptor ratio for the cortico-amygdala (left) and thalamo-amygdala (right) EPSCs recorded in slices from control and knockout mice. The ratio was calculated by dividing the amplitude of the AMPAR component measured at −70 mV by the amplitude of the NMDAR component measured 50 ms after the peak at +50 mV.

the induction procedure. Thus, the EPSP was potentiated to 147% ± 10% (8 cells) of its initial value in control slices. In contrast, the EPSP remained at 111.4% ± 12% (9 cells) of its baseline value when LTP-inducing stimulation was delivered in the presence of paclitaxel (see Figure S1A in the Supplemental Data available with this article online; significant difference, t test, $p < 0.05$). Paclitaxel in a concentration used had no detectable effect on either baseline AMPAR-mediated synaptic transmission or NMDAR-mediated synaptic responses (Figures S1B and S1C).

NMDA-Receptor Function Is Normal in *stathmin* Knockout Mice

Calcium influx through N-methyl-D-aspartate receptors (NMDARs) is required for the induction of LTP in afferent inputs to the LA (Huang and Kandel, 1998; Tsvetkov et al., 2004). Stathmin affects polymerization of tubulin dimers (Belmont and Mitchison, 1996). Tubulin in turn interacts with NMDA receptors (van Rossum et al., 1999) and thus could contribute to their synaptic targeting. Therefore, the reduction in LTP in the *stathmin* knockout could reflect a decrease in the NMDAR-mediated component of synaptic responses.

To address this possibility, we calculated an AMPA/NMDA ratio at the cortico-amygdala and thalamo-amygdala synapses (Tsvetkov et al., 2004) in slices from control and *stathmin* knockout mice. As shown in Figures 6E–6H, the AMPA/NMDA ratio in cortico-amygdala pathway was very similar in slices from control (14 cells, obtained from 5 control mice) and *stathmin* knockout mice (9 cells, obtained from 4 *stathmin* knockout mice; no significant difference, t test, $p = 0.81$). The AMPA/NMDA ratio at thalamo-amygdala synapses was also virtually identical in slices from control mice (7 cells, obtained from 3 control mice) and knockout mice (6 cells, obtained from 4 knockout mice; no significant difference, t test, $p = 0.9$; Figure 6H). Thus, the NMDAR function appears to be normal in *stathmin* knockout mice, suggesting that the effect of mutation on LTP was not mediated by changes in the NMDAR EPSC.

stathmin Knockout Mice Have Memory Deficits in Conditioned Fear

To investigate the relationship between changes in LTP and behavior, we turned to studying fear conditioning in *stathmin* knockout mice. Freezing increased immediately after the shock during training in both wild-type

and *stathmin* knockout mice (Figure 7A). The ANOVA revealed a significant effect of genotype with *stathmin* knockout mice showing a decreased level of freezing immediately after the shock [$F(1,46) = 4.896$; $p = 0.0319$]. Twenty-four hours later, in the same context, both groups of mice exhibited higher levels of freezing as compared to immediately after the shock, suggesting that they not only remembered the context where they received the electric shock the day before but also developed with time a strong aversive response to this environment associated to a painful experience (Figure 7A). The ANOVA revealed a significant effect of genotype [$F(1,46) = 5.329$; $p = 0.0255$] with the knockouts showing a lower response as compared to their controls. When placed in a new context 24 hr after training, mice displayed an increase in freezing at the onset of the tone (post-CS) as compared to their freezing level prior to the tone (session effect, all $p < 0.01$; Figure 7B). The ANOVA revealed a significant effect of genotype showing that the knockouts froze less than the wild-types at the presentation of the tone which had been associated previously with the electric shock [$F(1,46) = 4.565$; $p = 0.0380$].

We then analyzed pain sensitivity to the shock in the mutants (Figure 7C). No difference was found between groups (wild-type, n = 12; knockout, n = 10) in movement and jump in response to gradually increased levels of electric shock, which suggests that the deficits in fear conditioning were related to memory and not to pain sensitivity.

Innate Fear Is Deficient in *stathmin* Mutant Mice

We analyzed *stathmin* mutant mice for their anxiety levels using the open field and elevated plus maze. The open field represents a conflict test where mice placed in the novel environment naturally avoid the open space in the center of the arena (Figures 7D and 7E). Although *stathmin* knockout and wild-type mice displayed the same speed of locomotion, the ANOVA revealed that the mutants differed from the controls in the distance run in the aversive center of the field (significant effect of the interaction genotype x blocks [$F(11,308) = 4.116$; $p < 0.0001$]). A post hoc analysis revealed that the knockouts explored more of this environment than the controls at the beginning of the experiment (first six blocks, genotype effect [$F(1.28) = 4.484$; $p = 0.0432$]; Figure 7E). However, there was no difference in the exploration of the center of the arena at the end of the test or in the exploration of the periphery of the arena during the entire time.

We next examined anxiety levels of *stathmin* knockout mice in the elevated plus maze, where mice face a conflict between an aversion to the open arms of the maze and the motivation to explore these new areas (Figure 7F). The statistical analysis conducted on the number of entries in the closed arms did not reveal any significant effect of genotype. This result suggests that locomotor/exploratory activity in this environment was identical in both groups of mice in this apparatus. However, a difference was found in the number of entries in the open arms (significant effect of genotype [$F(1,28) = 4.349$; $p = 0.0463$]), with *stathmin* mutants making more entries in the open arms than their control littermates. In addition, statistical analysis conducted on the time spent in the open and closed arms revealed a significant effect of genotype (open arms [$F(1,28) = 6.892$; $p = 0.0139$]; closed arms [$F(1,28) = 13.041$; $p = 0.0012$]) indicating that the mutants were spending more time in the open compartment and less time in the closed arms than the controls were.

stathmin Knockout Mice Are Normal in Hippocampus-Dependent Spatial Memory

To explore potential changes in other types of memory in *stathmin* knockout mice, we examined their performance in the water maze, a task that is dependent on the hippocampus but not on the amygdala. Here, mice learn to remember the position of a hidden escape platform in a circular pool and are tested for their ability to navigate using distal cues surrounding the pool. During acquisition, mice from both groups showed a decrease in escape latency and path length (Figure 7G) across days, which indicates learning of the platform position (all groups, $p < 0.0001$). They also showed a preference for the target quadrant during the probe trial performed the last day of the experiment. We found no difference between groups in this task (no genotype effect), suggesting that the deletion of *stathmin* does not interfere with hippocampus-dependent learning and memory processes, which is consistent with lack of stathmin expression in the hippocampus of wild-type mice.

Discussion

Stathmin Is Positioned to Control Innate and Learned Fear

This study provides genetic evidence that amygdala-enriched stathmin is required for the expression of innate fear and the formation of memory for learned fear. We first found that stathmin is highly enriched in the LA, the main input of fearful information about the US and CS to the amygdala and the site of their convergence during fear learning. In addition, we found that the profile of expression of stathmin reflects the anatomy of the neural circuitry relaying fear-related information about the US and CS to the amygdala. The comparative analysis of the US and CS neural circuits leads to the conclusion that some of the US pathways are either overlapping or located proximally to those of the CS (Lanuza et al., 2004). Stathmin is expressed in most of the areas involved in processing of the tone CS, including the PIN and the MGN of the auditory thalamus, the TE3 area of the auditory cortex, and the perirhinal cortex. All these areas overlap with the US afferents of the amygdala. Stathmin is also expressed in the other areas processing the US, such as the somatosensory cortex, insular cortex, and posterior thalamus.

Because stathmin is a negative regulator of MT formation, we analyzed *stathmin* mutant mice for their ability to form MTs. Amygdala tissue in mice lacking stathmin has an increased amount of MTs, which may indicate more stable MTs and a decrease in the rate of MT dynamics (Westermann and Weber, 2003). Recent work provides important evidence in support of MT function in synaptic plasticity in *Drosophila* (Ruiz-Canada et al., 2004). MTs may be involved in synaptic activity in the mammalian brain by transporting different molecules and organelles to synapse proximity (Hiro-

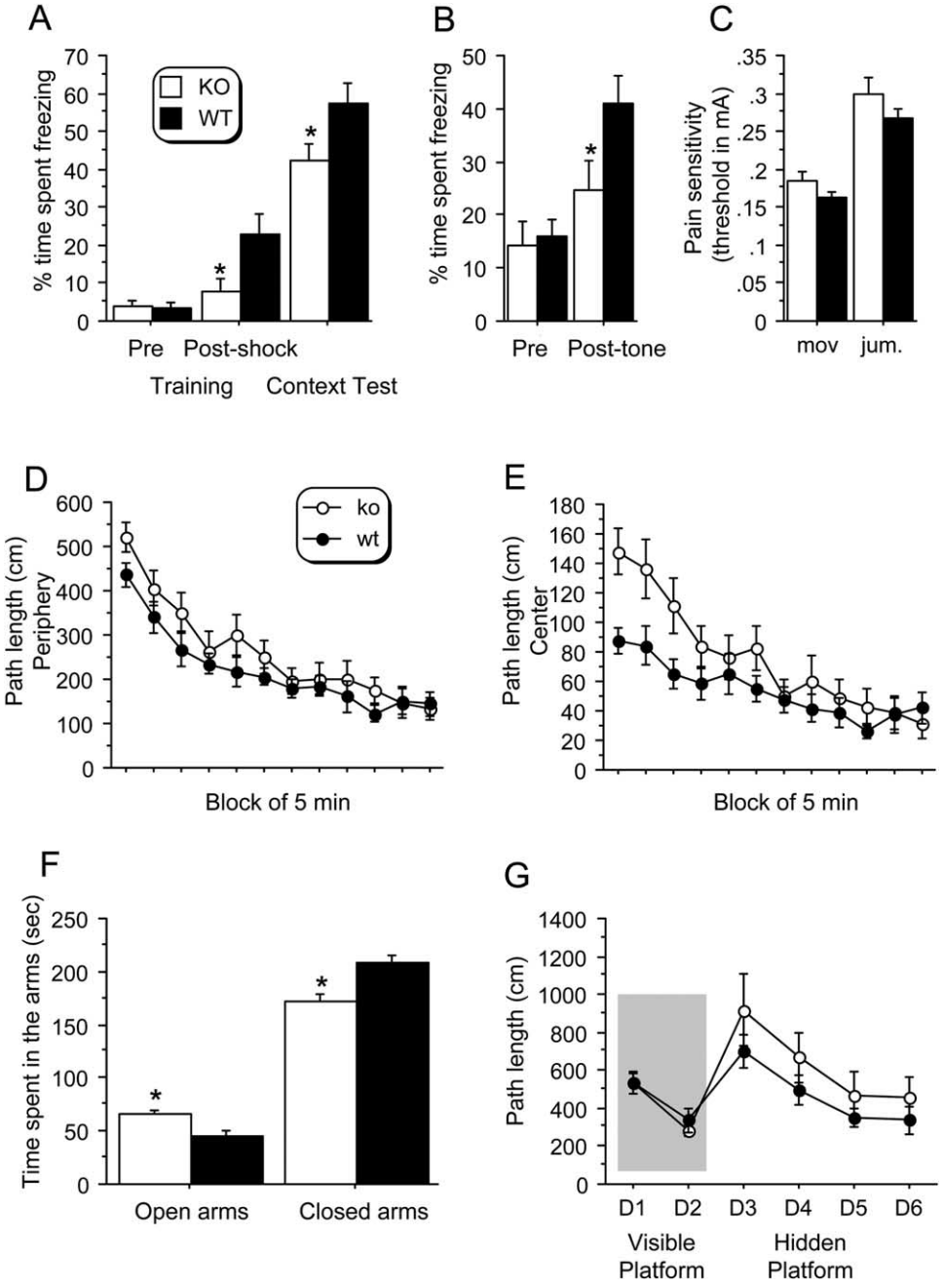

Figure 7. *stathmin* Knockout Mice Are Deficient in Fear Conditioning and Innate Fear

Error bars indicate SEM.

(A and B) *stathmin* knockouts (KO) froze less than wild-types (WT) in response to context or tone associated with foot shock. Significant difference in freezing responses between *stathmin* knockout mice (open bars) and wild-type mice (solid bars) was found immediately after the shock and 24 hr after training in both familiar ([A], Context Test) and new contexts in response to the tone ([B], Post-tone), although no difference was found between groups in the level of freezing before the onset of the tone ([B], Pre).

(C) Pain sensitivity. The intensities of the shock required to elicit movement (mov) and jump (jum) were assessed. No difference was found between groups.

(D–F) *stathmin* knockout mice have normal spatial memory but are deficient in innate fear.

(D and E) Open field: *stathmin* knockouts had the same path length in the periphery of the open-field box (D) but spent more time in the center of the box compared to the wild-types during the first half of the experiment (E).

(F) Elevated plus maze: *stathmin* knockout mice spent more time in the open arms and less time in the closed arms.

(G) *stathmin* knockout mice have normal spatial memory in the water maze. Both wild-type and *stathmin* knockout mice traveled the same distance to the platform in the visible (days 1 and 2, D1 and D2) and hidden versions (D3–D6) of the test.

kawa and Takemura, 2005). Indeed, we found that, even though both basic synaptic transmission and NMDAR function were normal, there was deficient LTP in both cortico-amygdala and thalamo-amygdala pathways in *stathmin* knockout mice. Also, in wild-type mice, in slices treated with taxol (which stabilizes MT), LTP was significantly decreased compared to the untreated slices.

Consistent with the LTP deficits, *stathmin* knockout mice were deficient in cued and contextual fear conditioning when tested 24 hr after training. The decrease in learned fear was not due to a general decrease in pain sensitivity or locomotor activity. In addition, experiments using the elevated plus maze and open field demonstrated that *stathmin* knockout mice displayed less anxiety than the controls. Thus, *stathmin* knockout mice display less fear in response to both learned and innate stimuli.

Our present and previous results (Shumyatsky et al., 2002) provide direct genetic evidence that LTP in the amygdala may serve as a mechanism for fear-related memory formation, thus supporting previous electrophysiological and behavioral observations (McKernan and Shinnick-Gallagher, 1997; Rogan et al., 1997; Tsvetkov et al., 2002). The behavioral phenotype observed in *stathmin* mutants is specifically associated with the amygdala-dependent fear behavior because *stathmin* knockout mice were normal in the water maze, suggesting that the deletion of stathmin does not interfere with hippocampus-dependent spatial memory.

Amygdala-Enriched Genes and the Circuit Specificity for Innate and Learned Fear

Interestingly, the role of stathmin in innate and learned fear contrasts with the role of the GRP/GRPR signaling pathway, which controls learned fear but not innate fear (Shumyatsky et al., 2002). Stathmin and GRP are both expressed in the LA and in the CS sensory afferents of the amygdala. Stathmin, however, is also expressed in the US neural circuitry where GRP is absent. The fact that both GRP and stathmin were originally isolated from the same single-cell cDNA library derived from a principal cell in the LA provides independent support for the fact that the neural circuitries for the US and CS converge in the LA. It is possible that a principal cell, from which the single-cell cDNA library was constructed (Shumyatsky et al., 2002), is an example of the subpopulation of pyramidal neurons in the LA that serve as the primary sites of convergence of the US and CS information and thus are the initial sites of fear memory formation.

The current models of fear memory formation suggest that US and CS convergence in the LA leads to an increase in synaptic strength in the afferent inputs to the LA, thus providing the necessary cellular basis for memory encoding (LeDoux, 2000; Maren, 2001). This is accompanied by the recruitment of the numerous intracellular processes, some of which are dependent on the proper function of MTs, including local events in the synapse that require protein and RNA transport to the synapse. This transport utilizes actin filaments (located in synapses) and MTs (located in axons and dendrites and maybe in synapses in limited quantities) as tracks by which cargo-transporting motor proteins move. Taken together, our work provides evidence for the possible role of MT dynamics in the regulation of innate and learned fear. Acting without the GRP/GRPR pathway, stathmin controls innate fear. However, acting in concert with the GRP/GRPR pathway, stathmin may control fear conditioning by regulating the ability of synapses in the neural circuitry of fear conditioning to undergo LTP.

More generally, these findings have several implications. To begin with, the evidence that stathmin is important in the regulation of fear suggests that *stathmin* knockout mice can be used as a model of anxiety states of mental disorders with innate and learned fear components. As a corollary, these animal models could be used to develop new antianxiety agents. Moreover, our previous results with GRPR knockout mice showing a selective alteration in learned fear and the present data showing that stathmin affects both innate and learned fear support the clinical data that indicate that anxiety is a spectrum of disorders that has a number of subclasses, each of which is likely to have a unique molecular signature and require distinctive pharmacological approaches.

Experimental Procedures

In Situ Hybridization and Immunocytochemistry

RNA in situ hybridization was performed as described (Schaeren-Wiemers and Gerfin-Moser, 1993). For Figure 1D, the NBT/BCIP substrate development was stopped earlier than in regular experiments to better demonstrate the difference between the images.

For colocalization experiments, the first of the two antibodies was visualized using horseradish-peroxidase-conjugated secondary antibody (Jackson ImmunoResearch) and fluorescein-labeled tyramide amplification reagent (1:100, Perkin Elmer). The second of the two antibodies was visualized by Cy3-conjugated secondary antibody (Jackson ImmunoResearch). Primary antibodies were mouse anti-NeuN (Chemicon), mouse anti-CaMKIIα (Chemicon), anti-GFAP (SMI22 clone), and rabbit anti-stathmin (Calbiochem).

Analysis of Microtubules and Synaptosomal Isolation

Analysis of Microtubules

MTs were isolated using a modification of the published procedure (Marklund et al., 1996). Amygdala tissue (8 mg) was collected in ice-cold PBS from 4- to 5-week-old control or mutant littermates. The tissue was homogenized in 400 μl of MT stabilizing buffer MTSB (0.1 M PIPES [pH 6.9], 2 M glycerol, 5 mM $MgCl_2$, 2 mM EGTA, 0.5% Triton X-100, 4 μg/ml Taxol, 5 μg/ml pefabloc SC [Fluka], 5 μg/ml leupeptin). The protein concentration was adjusted with MTSB to 2 μg/μl. Four hundred microliters of the brain lysate was spun at 40,000 × g for 20 min at 4°C to precipitate MT. The pellet was resuspended in 50 μl of water and 350 μl of MTSB. Each sample was boiled for 3 min and diluted with 1× sample buffer (50 mM Tris-HCl [pH 6.8], 2% SDS, 100 mM DTT, 10% glycerol, 0.01% bromophenol blue) and subjected to SDS-PAGE. Antibodies were against α-tubulin (Sigma), GAPDH (Chemicon), or stathmin (Calbiochem). Primary antibodies were visualized using ECF Kit (Amersham). Statistical analysis was performed by Student's t test.

Synaptosomal Isolation

All procedures were performed at 4°C to minimize proteolysis and MT assembly (Johnson et al., 1997). Cortico-amygdala tissue (120 mg) was collected from 18-week-old wild-type mice in modified Krebs-Henseleit buffer (mKRBS; 118.5 mM NaCl, 4.7 mM KCl, 1.18 mM $MgSO_4$, 2.5 mM $CaCl_2$, 1.18 mM KH_2PO_4, 24.9 mM $NaHCO_3$, 10 mM dextrose, 10 μg/ml adenosine deaminase, 5 μg/ml pefabloc SC [Fluka], 5 μg/ml leupeptin [pH 7.4]) and then homogenized in 1 ml of mKRBS containing 4 μg/ml Taxol (mKRBS-Taxol). The homogenate was diluted with 5 ml of mKRBS-Taxol, passed through 10

layers of nylon and then nitrocellulose, and finally was spun at 1000 × g for 15 min. The pellet was resuspended in 250 μl of MTSB. The protein concentration was adjusted to 5 μg/μl with MTSB. Antibodies were against PSD-95 (1:500), synaptophysin (1:500), CaMKII (Chemicon), MAP2 (Chemicon), and stathmin.

Two-Photon Microscopy

Two-photon laser scanning microscopy (TPLSM) was carried out using a Bio-Rad 1024-MP system with a Ti:sapphire laser (900 nm) (Spectra-Physics). Images were acquired using a 63× 0.9 NA water-immersion objective (Olympus) with Lasersharp software provided by Bio-Rad. Eight bit images of 512 × 512 pixels from the LA and hippocampus were collected, and Z series of 10–30 images taken at 1 μm steps were projected and aligned. Spines were identified and density of spines was determined by using software custom written in Interactive Data Language (IDL, Research Systems, Boulder, Colorado) as described previously (Lang et al., 2004).

Electrophysiology

Amygdala slices (250–300 μm) were prepared from control or *stathmin* knockout mice (littermates) with a vibratome. Slices were continuously superfused in solution containing (in mM) 119 NaCl, 2.5 KCl, 2.5 $CaCl_2$, 1.0 $MgSO_4$, 1.25 NaH_2PO_4, 26.0 $NaHCO_3$, 10 glucose, and 0.1 picrotoxin and equilibrated with 95% O_2 and 5% CO_2 (pH 7.3–7.4) at room temperature. Whole-cell recordings of evoked EPSCs were obtained from pyramidal cells in the LA under visual guidance (DIC/infrared optics) with an EPC-9 amplifier and Pulse v8.40 software (HEKA Elektronik). The EPSCs were evoked by stimulation of the fibers in either the external capsule (cortical input) or the internal capsule (thalamic input) at 0.05 Hz by a concentric stimulating electrode consisting of a silver-painted patch pipette (Tsvetkov et al., 2002, 2004). To elicit the evoked GABA-mediated IPSCs in the presence of CNQX (20 μM), the stimulation electrode was placed within the lateral nucleus of the amygdala. The patch electrodes (3–5 MΩ resistance) contained (in mM) 120 K-gluconate, 5 NaCl, 1 $MgCl_2$, 0.2 EGTA, 10 HEPES, 2 MgATP, and 0.1 NaGTP (adjusted to pH 7.2 with KOH). In recordings of $GABA_A$-receptor IPSCs, 120 mM of KCl was used instead of K-gluconate. To examine the voltage dependence of the EPSCs, 120 mM Cs-methane sulfonate was used instead of K-gluconate. Currents were filtered at 1 kHz and digitized at 5 kHz. In all LTP experiments, the stimulus intensity was adjusted to produce baseline synaptic responses with an amplitude that was ~20%–25% of maximum amplitude EPSP. Summary LTP graphs were constructed by normalizing data in 60 s epochs to the mean value of the baseline EPSP. The spontaneous miniature EPSCs were recorded in the presence of 1 μM tetrodotoxin and analyzed with the Mini Analysis Program (Synaptosoft Inc., Decatur, Georgia). All experiments on slices from control and knockout mice were performed blind to genotype.

Behavior

For all behavioral tasks, mutant and control littermates (males, 3 months old) were used. Statistical analyses used ANOVAs with genotype as the between-subject factor and session (fear-conditioning experiment), day, area (quadrant or platform in the Morris water maze), or zone (elevated plus maze) as within-subject factors. Mean ± SEM are presented. The experimenter was blind to the genotype in all studies. Mice were maintained and bred under standard conditions, consistent with the NIH guidelines and approved by the IACUC.

Fear Conditioning

On the training day, the mouse (wild-type, n = 25; knockout, n = 23) was placed in the conditioning chamber (Med Associates) for 2 min before the onset of the conditioned stimulus (CS), a tone that lasted for 30 s at 2800 Hz, 85 dB (Shumyatsky et al., 2002). The last 2 s of the CS was paired with the unconditioned stimulus (US), 0.7 mA of continuous foot shock. After an additional 30 s in the chamber, the mouse was returned to its home cage. Conditioning was assessed for 3 consecutive min in the chamber, in which the mice were trained by scoring freezing behavior, which was defined as complete lack of movement. Freezing was measured by a video-based system (Freezeframe, Actimetrics Software). Mice were tested immediately after training and at 24 hr after training. At 24 hr, testing occurred first in the context in which mice were trained (contextual fear conditioning). Three hours after, mice were placed in a novel environment in which the tone (120 s) that had been presented during training was given after a 1 min habituation period (pre-CS).

Water Maze

The task was performed as previously described (Shumyatsky et al., 2002), with two training phases: 2 days with a visible platform followed by 4 days (spatial phase) with a hidden platform in the training quadrant (wild-type, n = 15; knockout, n = 15). For each phase, four trials, 120 s maximum and 15 min ITI (intertrial interval), were given daily. Probe trials (60 s), during which the platform was removed, were performed to assess retention of the previously acquired information. The animals' trajectories were recorded with a videotracking system (HVS Image Analyzing VP-118).

Elevated Plus Maze

The elevated plus maze consisted of a center platform and four arms placed 50 cm above the floor (Shumyatsky et al., 2002). Two arms were enclosed within walls (15 cm) and the other two (open) had low rims (1 cm). Mice were placed in the center and their behavior was recorded for 5 min with a camera located above the maze (wild-type, n = 15; knockout, n = 15). Time spent (in seconds, sec) and entries in the different compartments (closed and open arms, center) were assessed.

Open Field

The open-field consisted of a white arena (40 cm × 40 cm × 40 cm) coupled to an automated video tracking system (wild-type, n = 15; knockout, n = 15). Mice were placed in the periphery of the arena, and the distance run and their speed were recorded over a 12 × 5 min (1 hr) period.

Foot-Shock Sensitivity

The procedure was done as described in Shumyatsky et al. (2002). The intensities of electric shock required to elicit movement and jump were determined for each mouse (wild-type, n = 12; knockout, n = 10) by delivering a 1 s shock every 30 s starting at 0.08 mA and increasing the shock 0.02 mA each time. Testing was stopped after all behaviors had been noted.

Supplemental Data

Supplemental Data include one figure and can be found with this article online at http://www.cell.com/cgi/content/full/123/4/697/DC1/.

Acknowledgments

We thank Steven Siegelbaum for support. We thank Joshua Sanes for providing EGFP-M mice. We thank Bonnie Firestein and Alexey Pronin for constructive discussions and Qiaoting Du for technical help. G.P.S. was supported by NARSAD, NAAR, the Cure Autism Now Foundation, and the New Jersey Governor's Council on Autism. E.R.K. was supported by NIMH grant MH50733, NIH Program Project grant on Amygdala and Anxiety States, and the G. Harold and Leila Y. Mathers Charitable Foundation. V.Y.B. was supported by the Whitehall Foundation, the Esther A. & Joseph Klingenstein Fund, NARSAD, and NIH grants NS44185 and DA15098. E.R.K. is a Senior Investigator of the HHMI.

Received: February 17, 2005
Revised: June 17, 2005
Accepted: August 26, 2005
Published: November 17, 2005

References

Amat, J.A., Fields, K.L., and Schubart, U.K. (1991). Distribution of phosphoprotein p19 in rat brain during ontogeny: stage-specific expression in neurons and glia. Brain Res. Dev. Brain Res. *60*, 205–218.

Belmont, L.D., and Mitchison, T.J. (1996). Identification of a protein that interacts with tubulin dimers and increases the catastrophe rate of microtubules. Cell *84*, 623–631.

Brunzell, D.H., and Kim, J.J. (2001). Fear conditioning to tone, but not to context, is attenuated by lesions of the insular cortex and

posterior extension of the intralaminar complex in rats. Behav. Neurosci. *115*, 365–375.

Campeau, S., and Davis, M. (1995). Involvement of subcortical and cortical afferents to the lateral nucleus of the amygdala in fear conditioning measured with fear-potentiated startle in rats trained concurrently with auditory and visual conditioned stimuli. J. Neurosci. *15*, 2312–2327.

Curmi, P.A., Andersen, S.S., Lachkar, S., Gavet, O., Karsenti, E., Knossow, M., and Sobel, A. (1997). The stathmin/tubulin interaction in vitro. J. Biol. Chem. *272*, 25029–25036.

Davis, M. (2000). The role of the amygdala in conditioned and unconditioned fear and anxiety. In The Amygdala, J.P. Aggleton, ed. (New York: Oxford University Press), pp. 213–287.

Fendt, M., and Fanselow, M.S. (1999). The neuroanatomical and neurochemical basis of conditioned fear. Neurosci. Biobehav. Rev. *23*, 743–760.

Feng, G., Mellor, R.H., Bernstein, M., Keller-Peck, C., Nguyen, Q.T., Wallace, M., Nerbonne, J.M., Lichtman, J.W., and Sanes, J.R. (2000). Imaging neuronal subsets in transgenic mice expressing multiple spectral variants of GFP. Neuron *28*, 41–51.

Gavet, O., El Messari, S., Ozon, S., and Sobel, A. (2002). Regulation and subcellular localization of the microtubule-destabilizing stathmin family phosphoproteins in cortical neurons. J. Neurosci. Res. *68*, 535–550.

Hanash, S.M., Strahler, J.R., Kuick, R., Chu, E.H., and Nichols, D. (1988). Identification of a polypeptide associated with the malignant phenotype in acute leukemia. J. Biol. Chem. *263*, 12813–12815.

Hirokawa, N., and Takemura, R. (2005). Molecular motors and mechanisms of directional transport in neurons. Nat. Rev. Neurosci. *6*, 201–214.

Huang, Y.Y., and Kandel, E.R. (1998). Postsynaptic induction and PKA-dependent expression of LTP in the lateral amygdala. Neuron *21*, 169–178.

Johnson, M.W., Chotiner, J.K., and Watson, J.B. (1997). Isolation and characterization of synaptoneurosomes from single rat hippocampal slices. J. Neurosci. Methods *77*, 151–156.

Kaech, S., Parmar, H., Roelandse, M., Bornmann, C., and Matus, A. (2001). Cytoskeletal microdifferentiation: a mechanism for organizing morphological plasticity in dendrites. Proc. Natl. Acad. Sci. USA *98*, 7086–7092.

Lang, C., Barco, A., Zablow, L., Kandel, E.R., Siegelbaum, S.A., and Zakharenko, S.S. (2004). Transient expansion of synaptically connected dendritic spines upon induction of hippocampal long-term potentiation. Proc. Natl. Acad. Sci. USA *101*, 16665–16670.

Lanuza, E., Nader, K., and Ledoux, J.E. (2004). Unconditioned stimulus pathways to the amygdala: effects of posterior thalamic and cortical lesions on fear conditioning. Neuroscience *125*, 305–315.

LeDoux, J.E. (2000). Emotion circuits in the brain. Annu. Rev. Neurosci. *23*, 155–184.

Mahanty, N.K., and Sah, P. (1998). Calcium-permeable AMPA receptors mediate long-term potentiation in interneurons in the amygdala. Nature *394*, 683–687.

Majak, K., Pikkarainen, M., Kemppainen, S., Jolkkonen, E., and Pitkanen, A. (2002). Projections from the amygdaloid complex to the claustrum and the endopiriform nucleus: a Phaseolus vulgaris leucoagglutinin study in the rat. J. Comp. Neurol. *451*, 236–249.

Maren, S. (2001). Neurobiology of Pavlovian fear conditioning. Annu. Rev. Neurosci. *24*, 897–931.

Maren, S., and Quirk, G.J. (2004). Neuronal signalling of fear memory. Nat. Rev. Neurosci. *5*, 844–852.

Marklund, U., Larsson, N., Gradin, H.M., Brattsand, G., and Gullberg, M. (1996). Oncoprotein 18 is a phosphorylation-responsive regulator of microtubule dynamics. EMBO J. *15*, 5290–5298.

McDonald, A.J., Muller, J.F., and Mascagni, F. (2002). GABAergic innervation of alpha type II calcium/calmodulin-dependent protein kinase immunoreactive pyramidal neurons in the rat basolateral amygdala. J. Comp. Neurol. *446*, 199–218.

McGregor, I.S., Hargreaves, G.A., Apfelbach, R., and Hunt, G.E. (2004). Neural correlates of cat odor-induced anxiety in rats: region-specific effects of the benzodiazepine midazolam. J. Neurosci. *24*, 4134–4144.

McKernan, M.G., and Shinnick-Gallagher, P. (1997). Fear conditioning induces a lasting potentiation of synaptic currents in vitro. Nature *390*, 607–611.

Rodrigues, S.M., Schafe, G.E., and LeDoux, J.E. (2004). Molecular mechanisms underlying emotional learning and memory in the lateral amygdala. Neuron *44*, 75–91.

Rogan, M.T., Staubli, U.V., and LeDoux, J.E. (1997). Fear conditioning induces associative long-term potentiation in the amygdala. Nature *390*, 604–607.

Ruiz-Canada, C., Ashley, J., Moeckel-Cole, S., Drier, E., Yin, J., and Budnik, V. (2004). New synaptic bouton formation is disrupted by misregulation of microtubule stability in aPKC mutants. Neuron *42*, 567–580.

Schaeren-Wiemers, N., and Gerfin-Moser, A. (1993). A single protocol to detect transcripts of various types and expression levels in neural tissue and cultured cells: in situ hybridization using digoxigenin-labelled cRNA probes. Histochemistry *100*, 431–440.

Schubart, U.K., Xu, J., Fan, W., Cheng, G., Goldstein, H., Alpini, G., Shafritz, D.A., Amat, J.A., Farooq, M., and Norton, W.T. (1992). Widespread differentiation stage-specific expression of the gene encoding phosphoprotein p19 (metablastin) in mammalian cells. Differentiation *51*, 21–32.

Schubart, U.K., Yu, J., Amat, J.A., Wang, Z., Hoffmann, M.K., and Edelmann, W. (1996). Normal development of mice lacking metablastin (P19), a phosphoprotein implicated in cell cycle regulation. J. Biol. Chem. *271*, 14062–14066.

Shi, C., and Davis, M. (1999). Pain pathways involved in fear conditioning measured with fear-potentiated startle: lesion studies. J. Neurosci. *19*, 420–430.

Shumyatsky, G.P., Tsvetkov, E., Malleret, G., Vronskaya, S., Hatton, M., Hampton, L., Battey, J.F., Dulac, C., Kandel, E.R., and Bolshakov, V.Y. (2002). Identification of a signaling network in lateral nucleus of amygdala important for inhibiting memory specifically related to learned fear. Cell *111*, 905–918.

Tonegawa, S., Nakazawa, K., and Wilson, M.A. (2003). Genetic neuroscience of mammalian learning and memory. Philos. Trans. R. Soc. Lond. B Biol. Sci. *358*, 787–795.

Tsvetkov, E., Carlezon, W.A., Benes, F.M., Kandel, E.R., and Bolshakov, V.Y. (2002). Fear conditioning occludes LTP-induced presynaptic enhancement of synaptic transmission in the cortical pathway to the lateral amygdala. Neuron *34*, 289–300.

Tsvetkov, E., Shin, R.M., and Bolshakov, V.Y. (2004). Glutamate uptake determines pathway specificity of long-term potentiation in the neural circuitry of fear conditioning. Neuron *41*, 139–151.

van Rossum, D., and Hanisch, U.K. (1999). Cytoskeletal dynamics in dendritic spines: direct modulation by glutamate receptors? Trends Neurosci. *22*, 290–295.

van Rossum, D., Kuhse, J., and Betz, H. (1999). Dynamic interaction between soluble tubulin and C-terminal domains of N-methyl-D-aspartate receptor subunits. J. Neurochem. *72*, 962–973.

Westermann, S., and Weber, K. (2003). Post-translational modifications regulate microtubule function. Nat. Rev. Mol. Cell Biol. *4*, 938–947.